https://doi.org/10.1016/j.renene.2018.04.070

Development of an inline vertical cross-flow turbine for hydropower harvesting in urban water supply pipes

Du Jiyun, Yang Hongxing*, Shen Zhicheng, Guo Xiaodong

Renewable Energy Research Group, Department of Building Services Engineering, The Hong Kong Polytechnic University, Hong Kong, China

Corresponding author email: Hong-xing.yang@polyu.edu.hk

Abstract

Continuous and reliable power supply plays an important role for water leakage monitoring systems used in urban water supply pipes. Renewable energies powered water leakage monitoring system is becoming a promising way to reduce the dependence on traditional chemical batteries. In this study, an inline vertical cross-flow turbine was developed to harvest the potential hydropower inside water supply pipes for supplying power to the water monitoring systems. Specifically, numerical investigations are carried out on the block shapes of a water turbine system to determine an optimal model. The effects of tip clearance on the turbine performance are conducted and it is found that a smaller tip clearance can reduce the reversing torque on the returning blades and increase the pressure drop through the runner for improving the turbine performance. Besides, a self-adjustable vane is designed to avoid excess water head loss. The simulation results show that the proposed self-adjustable vane can limit the water head loss at high flow velocities (1.5-2.0 m/s) to 5m. Finally, the turbine prototype is fabricated and tested on a lab test rig. The experimental results indicate that the numerical method adopted in this research is accurate enough for such micro water turbine performance predictions. A month-long test shows that the daily electricity generation of the proposed turbine is about 600Wh and the water head loss is always below 5m, which means that the proposed turbine can provide sufficient power for any general water leakage monitoring system without influencing normal water supply.

Keywords: Water leakage monitoring system; urban water supply; micro hydropower;

inline cross-flow turbine; tip clearance; self-adjustable vane

1. Introduction

Water leakage has been a huge challenge for urban water supply because of the rapid deterioration of pipelines [1]. Taking Hong Kong for instance, most of the water pipelines are laid 30 years ago, it is estimated that nearly 25% of the fresh water is wasted due to pipe leakage [2,3]. Therefore, many technologies, such as noise monitoring, flow and pressure monitoring, are developed for timely detection and early warning of water leakage [4,5]. To apply these technologies, lots of different sensors and meters are installed at different nodes to collect data for leakage inspections [5]. Traditionally, these meters and sensors are powered by chemical batteries, which usually have limited lifespans even with efficient energy conserving mechanisms [6]. Once the batteries ran out, the monitoring system would die, so the batteries need to be replaced frequently, resulting in a high cost and a huge demand for labor [7]. For this reason, interests in developing leakage monitoring system powered by constant renewable energy sources are growing rapidly.

In the current research, several different renewable energy sources (i.e. vibration, solar energy and wind energy) are adopted to provide power for leakage monitoring system [8,9,10,11]. However, there are several drawbacks of these renewable sources. Firstly, these power sources are uncontrollable and not steadily available, so they cannot be harvested whenever wanted [12]. On the other hand, their energy harvesters are usually bulky and therefore need more space to install. But most of the water monitoring sensors and meters are usually located underground or limited spaces that surrounded by trees or buildings in the urban areas, which significantly restricts the application of these renewable sources. Actually, the most available and steady renewable source for water pipe leakage monitoring system is the potential hydropower inside the water pipes. Usually, the water pressure in the urban water supply pipes is usually very high and even excess (50-80m water) to ensure normal water supply through the whole urban

area, so it is a promising way to harvest the excess hydropower for power supply to the leakage monitoring system. Some studies have been done to harness the hydropower inside the water supply pipelines. Hao [13] developed a self-powered flowmeter that integrated with a runner and a micro generator, so the meter could harvest hydropower from the pipes and needs no batteries. Similar design could also be found in the report of Hoffmann [14]. However, these techniques possess a requirement for the structure modification of sensors or meters, which is likely to be challenging for the whole leakage monitoring system with thousands of nodes.

In the past decades, micro hydropower technologies in the domains of remote power supply, pumped storage power plant and industrial hydropower recovery have been very mature, but micro hydropower generation in water supply pipes has been less studied and is still at the developmental stage [15,16]. The main challenge of hydropower generation in water supply pipes is the selection or design of proper turbines that can meet the requirement of water supply. The requirements are as followed:

1) The generated electricity should meet the power demand of water monitoring system, but too much power may possess a huge load on the energy control and storage system. Based on the data provided by the Water Supplies Department of Hong Kong, 40-100W power is sufficient for nearly any water monitoring system.

2) Although there exists some excess water head in the water pipes, the turbine cannot consume too much water head. To avoid negative effects on the normal water supply through the whole urban area, the consumed water head cannot exceed 5m water.

3) As most urban water pipes are laid underground, the installation space is very limited and the modification of the pipes should be as slight as possible.

4) The most important thing is that the application of water turbine cannot have bad impact on the water quality.

There are many kinds of micro hydro turbines that suitable for different water head and flow rate. Generally, micro hydro turbines are divided into impulse turbine (i.e. Pelton, Turgo and crossflow turbines) and reaction turbines (i.e. Francis turbine, propeller turbine and pump as turbine) based on their working principle [16]. Among these turbines, the crossflow turbine and propeller turbines could operate under a low water head and high water flow rate [17]. However, the inlet and outlet of the traditional propeller turbine are orthogonal [18], which means that the application of propeller turbine will need to modify the flow path of water pipes. Although the bulb propeller turbine could be used inside the water pipes without changing the flow path [19,20,21], the generator and other electrical components are all submerged in the drinking water, any failure of waterproof may result in severe water pollution. In the previous research of our research group, a pico cross-flow turbine with a spherical rotor was developed for hydropower harvesting in DN100 water pipelines and achieved a good performance [1]. Nevertheless, the turbine is designed for water supply pipelines in high rise buildings and cannot be used in the water mains, where the pipe diameter is much larger.

To solve the problem related to hydropower harvesting in water pipes, a project aiming to develop an inline vertical cross-flow turbine for electricity generation in the urban water pipes with diameters of 200-250mm was supported by the Water Supplies Department of Hong Kong. This paper aims to present the design process by numerical methods and the turbine performance obtained from on-site tests.

2. Methodology

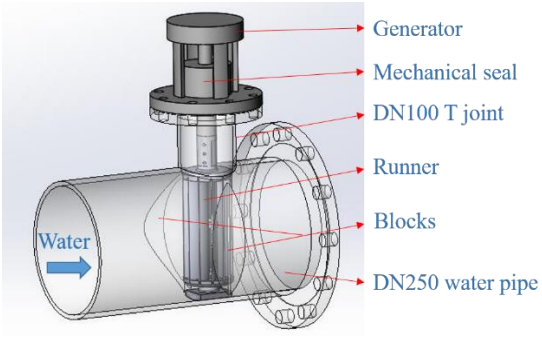

Fig.1 The turbine design scheme

To satisfy the requirements mentioned earlier, a turbine design scheme as shown in Figure 1 was proposed. The main idea of this scheme is to integrate a DN100 T-joint to the DN250 pipe, then a cross-flow runner, which connects with a generator via a shaft, is inserted in the pipe through the T-joint to harvest hydropower and transfer the power to the generator. After that, the generated electricity will be stored in chargeable batteries after rectification. As suggested in our previous research, blocks that fixed on the pipe inner wall are necessary because the blocks can let more water to flow through the runner, increasing the velocity of water that passes through the runner and reducing the resistance of water on the returning blades [1].

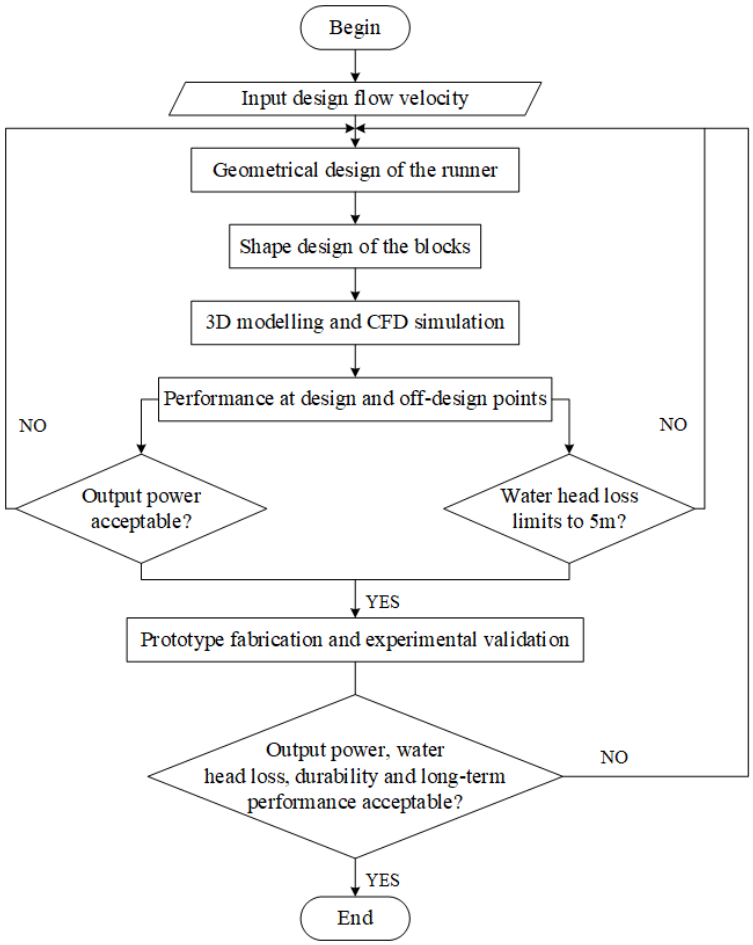

Fig.2 The research flow chart

The entire research flow chart is indicated in Figure 2. The flow velocity inside the urban water mains is about 1.2-2.0m/s and the average velocity is about 1.5m/s [1]. So the design flow velocity on the design point is set as 1.5 m/s. As shown in Figure 2, the

turbine design starts with the calculation of the runner geometrical parameters and the shape design of the blocks. After that, the 3D models of different design will be built and the optimal model is obtained by computational fluid mechanics (CFD) simulations. Finally, the prototype is fabricated and on-site tests are conducted to validate the numerical results and study the turbine performance. The design process would be repeated if the numerical or experimental results do not satisfy the design requirements.

2.1 Geometrical parameters

The key part of the cross-flow turbine is the runner and its main geometrical parameters are indicated in Figure 3. Among these parameters, the length L and the outer diameter of the runner D_1 are determined by the diameters of water pipe and T joint respectively. Besides, the runner inner diameter D_2, the blade outer angles β_1 and inner angle β_2 are determined based on the optimal values suggested by Vincenzo Sammartano [22], and the geometrical parameters are listed in Table 1. In the present paper, the shape of blocks is designed mainly by CFD simulation.

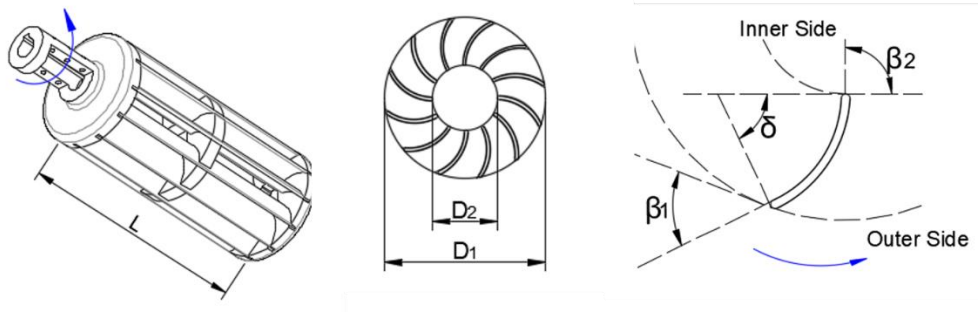

Fig.3 The main geometrical parameters of the cross-flow runner

Table 1 The values of runner main geometrical parameters

Geometrical Parameters	Symbols	Values
Blade outer angle	β_1	42°
Blade inner angle	β_2	90°
Outer diameter	D_1	98mm
Inner diameter	D_2	45mm
Runner length	L	215mm

2.2 CFD setting

In recent years, the CFD methods have been widely used as powerful and promising tools in turbomachinery design, performance prediction and optimization [23,24,25]. In the present paper, the CFD method is used to study the effect of different block shapes on the turbine performance and the inside flow field characteristics.

2.2.1 Meshing

The physical model of the turbine, which is composed of four main parts: inlet extension part, turbine body, runner and outlet extension part, was built in SolidWorks 2014, a three-dimensional modeling computer-aided design software. As the computational domain can be regarded as symmetric, only half of the model was built to reduce the computing time. Then the physical model was imported into ICEM CFD 14.5 for unstructured tetrahedral grids generation. The whole computational domain was separated into two main domains: stationary domain and rotary domain. Inlet extension part, turbine body and outlet extension part belong to the stationary domain while runner is the rotary domain. For simulation, the sliding-mesh interface method was adopted to allow for the mesh motion between static and rotating parts [26,27]. In the meshing process, the “tetra mesh” was employed to generate grids in the domains far from boundaries, while the “prism mesh” was used for grid generation in the domains near boundaries, i.e. the pipe wall and blades. Such strategy could achieve a good balance between calculation time and accuracy. To minimize the numerical uncertainty in the solution, a grid independence test was conducted. Six meshing schemes were tested and their grid numbers are 0.63, 1.09, 1.5, 1.91, 3.78 and 9.6 million respectively. Figure 4 shows the dependence of shaft power on the grid number, according to the results, the total grid number of 1.91 million was taken for the next study. The final computational mesh is showed in Figure 5.

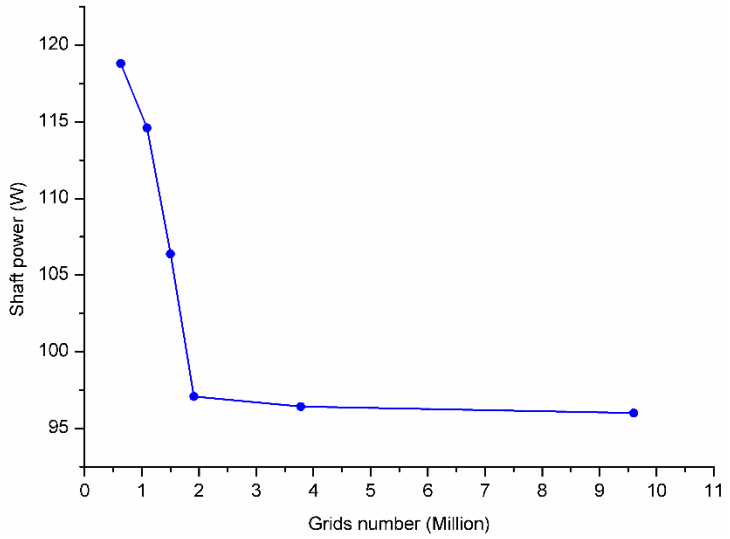

Fig.4 The dependence of shaft power on the grid number

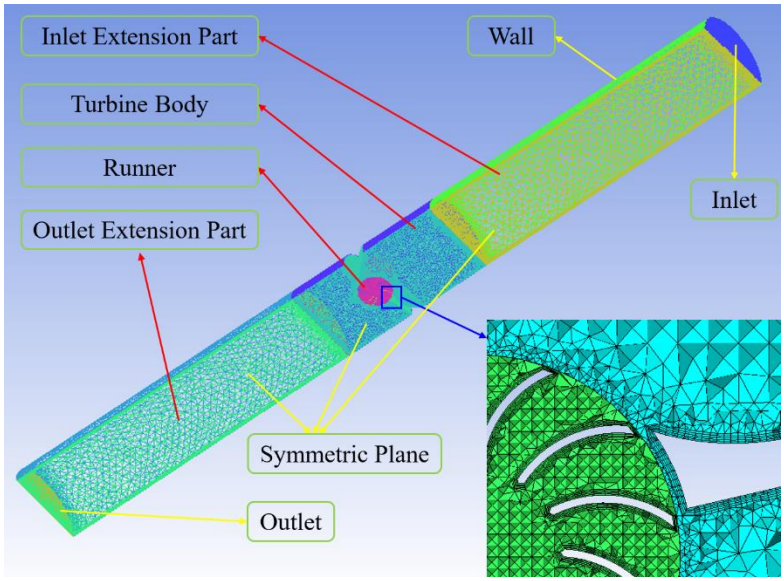

Fig.5 The final meshing scheme

2.2.2 Solver setup

The incompressible isothermal flow through a turbomachine is fully described by the continuity and momentum equations, which are called the Navier-Stokes equations and written as:

$$\frac{\partial u_i}{\partial x_i} = 0 \tag{1}$$

$$\frac{\partial u_i}{\partial t} + u_j \frac{\partial u_i}{\partial x_j} = -\frac{1}{\rho}\frac{\partial p}{\partial x_i} + \nu \frac{\partial^2 u_i}{\partial x_i \partial x_j} \tag{2}$$

where u is the velocity, p is the pressure, ν is the kinematic viscosity of fluid, ρ is the density of fluid.

Since solving the Navier-Stokes equations is computationally expensive for high Reynolds number flows in complex geometries, the Reynolds averaged Navier–Stokes (RANS) equations are generally solved to determine the mean velocity field. RANS equations are obtained by time-averaging the Navier-Stokes equations for the mean values of the flow variables over a sufficiently long period compared to the frequencies of turbulent fluctuations, and are written as:

$$\frac{\partial U_i}{\partial x_i} = 0 \tag{3}$$

$$\frac{\partial U}{\partial t} + U_j \frac{\partial U_i}{\partial x_j} = -\frac{1}{\rho}\frac{\partial P}{\partial x_i} + \frac{\partial}{\partial x_j}\left[\nu\left(\frac{\partial U_j}{\partial x_i} + \frac{\partial U_i}{\partial x_j}\right) - \overline{u_i' u_j'}\right] \tag{4}$$

where U is the time-averaged velocity, u_i' is the fluctuating velocity due to turbulence and $\rho\overline{u_i' u_j'}$ is the Reynolds shear stress.

RANS simulations with appropriate turbulence models have been widely used for turbomachinery design analyses due to their low computational cost and satisfactory predictive capability for average device performance [28,29]. In this study, the SST $k-\omega$ model is used because the SST $k-\omega$ model combines the standard $k-\omega$ model and standard $k-\varepsilon$ model, it takes the effects of turbulence shear stress into consideration in the definition of the turbulence viscosity and could capture the micro flow in the viscous layer.

The simulations were conducted in ANSYS Fluent 14.5 using a second-order-accurate finite-volume discretization scheme and the maximum residual is set to 10^{-5}. The inlet velocity is considered as the inlet boundary condition of the inlet face while the outlet

boundary condition is set as pressure outlet with the pressure equal to atmospheric pressure. The boundary condition of turbine wall and blades is set as non-slip smooth wall. Besides, the boundary condition of symmetric plane is set as symmetry.

2.3 Experimental setup

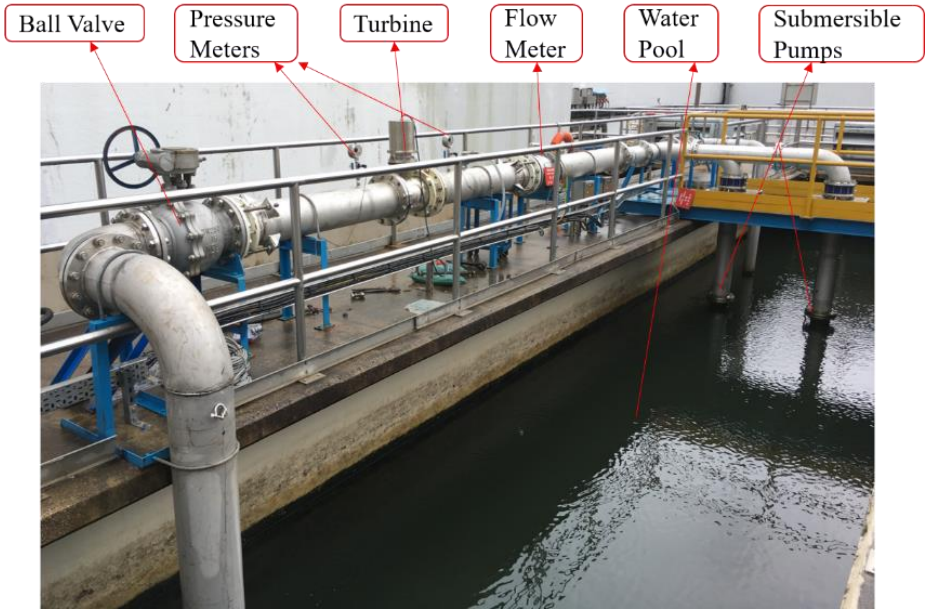

Fig.6 The hydraulic test rig at the MOSWTW

After a series of simulations, the main structure and components were determined and a prototype was fabricated. The turbine prototype was installed in a hydraulic test rig built based on a carbon contact chamber at Ma On Shan Water Treatment Works (MOSWTW) of Hong Kong to test its performance. Figure 6 indicates the diagram of the hydraulic test rig, which is mainly composed of two parallel submersible pumps, DN250 water pipes, the water turbine, two pressure meters, an electromagnetic flow meter, an adjustable ball valve and a frequency converter controller. The submersible pumps can provide 80m water head at 530m^3/h (3m/s in DN250 water pipes) to analogize the real flow conditions inside the urban water supply pipes. The working load of the submersible pumps is controlled by the frequency converter controller, by adjusting the working frequency of the submersible pumps and the opening degree of the ball valve, different flow velocity and water head can be achieved in the test rig. A

24V three-phase permanent magnet alternating generator with low starting torque is chose to translate shaft power of the turbine into electric energy. Besides, two pressure meters are used to examine the pressure drop between the upstream and downstream of the water turbine. In the described test rig, the electromagnetic flow meter has a precision of ±0.5% full scale while the precision of pressure meter is ±0.25% full scale. Using the prescribed methods for uncertainty estimation [30], the composite errors for water head loss and efficiency measurement are ±0.25% and ±0.56%, respectively.

An electricity control and storage system was developed to manage the generated power. As shown in Figure 7, the electricity control and storage system is mainly composed of controller, two 12V chargeable batteries, dump load and computer. Electricity generated by the permanent magnet alternating generator is rectified in the controller then stored in the chargeable batteries. Once the charging voltage is higher than the bearable voltage of batteries, the dump load will be used to consume excess electricity. The Flow velocities, output power, charging current and voltage and the pressure difference can be monitored and recorded in the computer.

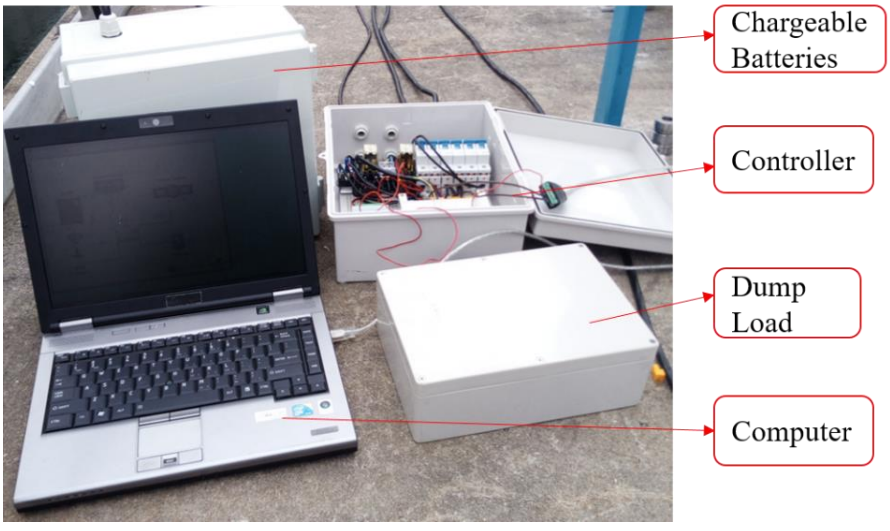

Fig.7 The electricity control and storage system

2.4 Data analysis

To assess the turbine performance, both the numerical and experimental output power and water head loss should be monitored. The experimental results can be obtained directly based on the data collected in the remote monitoring computer, but some calculation is needed to get the numerical results. In the CFD simulation, the output torque of the runner is recorded and the shaft power of the turbine is calculated by Equation (5). For the calculation of actual output power, mechanical loss and generator conversion efficiency must be considered as energy loss is inevitable in energy conversion process, as shown in Equation (6).

$$P_{shaft} = T\omega \tag{5}$$

$$P_s = \eta_{me}\eta_g P_{shaft} \tag{6}$$

where P_{shaft} is the shaft power (W), ω is the rotational speed (rad/s), T is the shaft torque (N·m), P_s is the actual simulation power output (W), η_{me} is the overall mechanical efficiency, and η_g is the conversion efficiency of generator. In this study, the mechanical efficiency and generator conversion efficiency are determined based on the data provided by parts suppliers.

The CFD simulations were conducted to study the turbine performance on the design points and off-design points. For performance study on the design points, the tip speed ratio (TSR) was introduced. The TSR means the ratio of the peripheral speed of the turbine runner and the flow velocity and it can be calculated using Equation (7). By varying the values of ω, different TSRs can be obtained. Correspondingly, by changing the rotation speed in the simulation setup, different output power and water head loss for different TSRs can be acquired. Finally, by changing the inlet velocity of simulation setup, the turbine performance at off-design points were obtained.

$$TSR = \frac{r\omega}{V} \tag{7}$$

where r is the runner radius (m); V is the flow velocity (m/s).

In the experimental process, the flow velocity, charging voltage and current, water head of upstream and downstream can be transmitted to the controller and recorded in the monitoring computer, so the experimental results can be finally acquired by simple calculations.

3. Numerical results and analysis

In our previous research, it has been found that the negative torque generated by returning blades had an opposite impact on the performance of cross-flow turbine [1]. Many investigations have indicated that placing a block or inlet nozzle on the inlet side of the runner can decrease the water resistance which exerts on the returning blades, thus the performance of cross-flow turbine can be improved [31,32]. In this research, the CFD simulations were conducted to investigate the effects of different blocks on the performance of inline cross-flow turbine and further find the optimal block model.

3.1 The design of block shape

Four block models with different geometrical design (as shown in Figure 8) were built and simulated to study the impact of different block shapes on the turbine performance. In Case 1, one block with concave surface is integrated in the pipe inner wall on the upstream side while one block with convex surface is placed on the same location in Case 2. Compared to Case 1 and 2, one block with plane surface is added in Case 3 and 4, respectively.

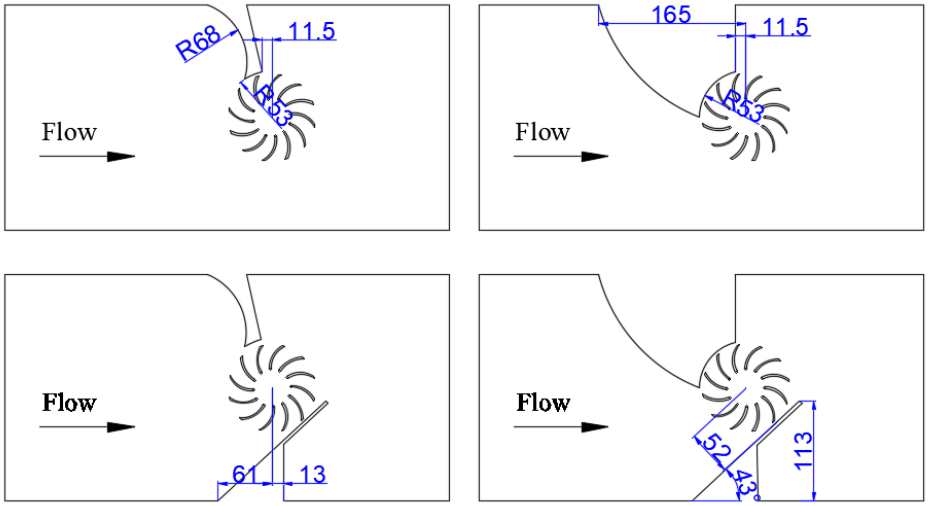

Fig.8 Different block models

The output power and water head loss of the turbine on design point and off-design points are recorded to obtain the characteristics of turbine performance. Figure 9 and Figure 10 illustrate the output power and water head loss through the turbine for different TSR on the design point. As shown in Figure 9, the output power of Case 1 and Case 2 increases with the increment of TSR until reach maximum values, then decrease. The maximum output power of Case 1 and Case 2 occurs where the TSR is 0.9 and 1.1, respectively. The output power of both Case 3 and Case 4 also increases with the increment of TSR, but the increase trend of Case 4 is more obvious than that of Case 3. For water head loss through the turbine, all the four cases experience a slight growth with the TSR and all the values are lower than 5m water, which means that all the cases can meet the requirement from the aspect of water head loss at the design point. Table 2 compares the maximum output power and the corresponding TSR and water head loss of the four cases. Case 1 and Case 2 indicate poor performance in comparison with other two cases, the main reason for the poor performance can be explained by the velocity vectors as shown in Figure 11. It can be seen that although the upstream block can modify the flow path and force more water to flow through the runner, most of the water flows away without doing any work on the blades due to the absence of downstream block. By adding downstream blocks in Case 3 and Case 4, the

upstream and downstream blocks can act as convergence nozzles while the downstream pipe can function as a diffuser. As indicated in the velocity vectors of Case 3 and Case 4, the highest velocity regions are observed in the domain of runner and the velocity behind the runner is reduced, therefore the total harvested power from water flow raises significantly. Both the Case 3 and Case 4 possess a good performance, but compared to Case 3, Case 4 indicates a good performance in terms of output power. This is mainly due to the smaller inlet discharge area and bigger cover area on the returning blades in Case 4. A small inlet discharge area usually corresponds to a higher flow velocity towards the advancing blades, so more energy can be harnessed by the runner. On the other hand, a bigger cover area on the returning blades can reduce the influence of negative torque on the turbine performance. It can be observed in Figure 10 that the water head loss of Case 3 is the highest among all the cases. This is because that the upstream block with concave surface in Case 3 changes the flow direction sharply, which may cause severe hydraulic loss.

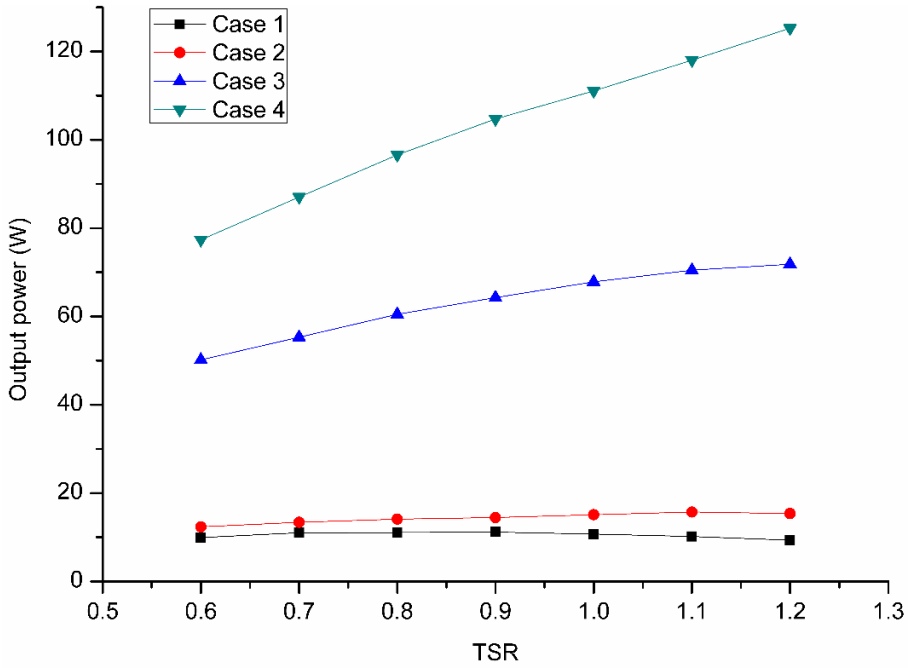

Fig.9 The output power of four cases with different TSR

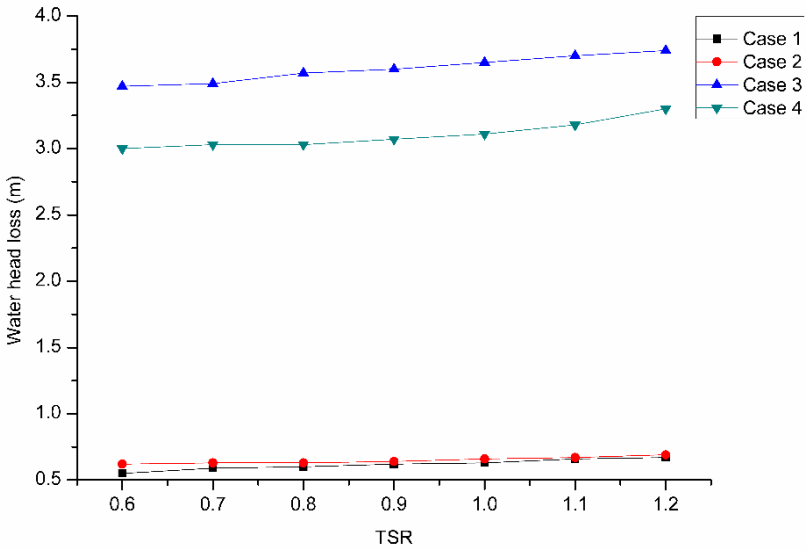

302

303 Fig.10 The water head loss of four cases with different TSR

304 Table 2 Simulated results of four cases on the design point

No.	Description	Max power (W)	Water head loss (m)	TSR
Case 1	Upstream concave block	11.2	0.62	0.9
Case 2	Upstream convex block	15.7	0.67	1.1
Case 3	Upstream concave block and downstream plane block	71.8	3.74	1.2
Case 4	Upstream convex block and downstream plane block	125.2	3.3	1.2

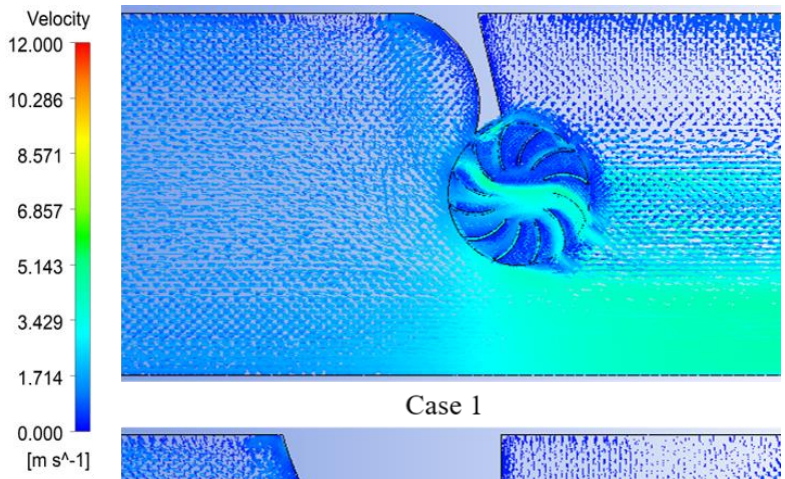

Case 1

Case 2

Case 3

Case 4

305

306 Fig.11 The velocity vectors of different cases

Furthermore, it can be seen in the Figure 11 that water leakage occurs in the tip clearance between the blades and the upstream block. The water leakage would not only increase friction losses, but also produce negative torque on the blades, leading to significant performance degradation. The optimal tip clearance as determined in the followed part.

Figure 12 and 13 show the variation of output power and water head loss with respect of flow velocities on the off-design points. It is noticed that the output power and water head loss of all the cases experience an increase with the increase of flow velocities. However, the performance of Case 1 and Case 2 is still very poor even at a high flow velocity, so these two cases are abandoned in the project. Case 4 indicates the highest output power among all the cases, but its output power at high flow velocities (1.7m/s and above) is so high that may exceed the tolerance of the 24V controller, which is used to rectify and store the generated electricity and to monitor the working conditions of the turbine. By contrast, Case 3 possesses a modest increase with the flow velocities and its output power at 2m/s is about 135W, which meets the security requirement of the controller very well. From the aspect of water head loss, both the Case 3 and Case 4 exceed 5m water head at high flow velocities, this problem can be solved by introducing a self-adjustable vane, which will be studied in the followed parts. To sum up, although the output power of Case 4 is better than that of Case 3, it is not the most suitable configuration for this project and the Case 3 will be selected as the optimal model for next step of research.

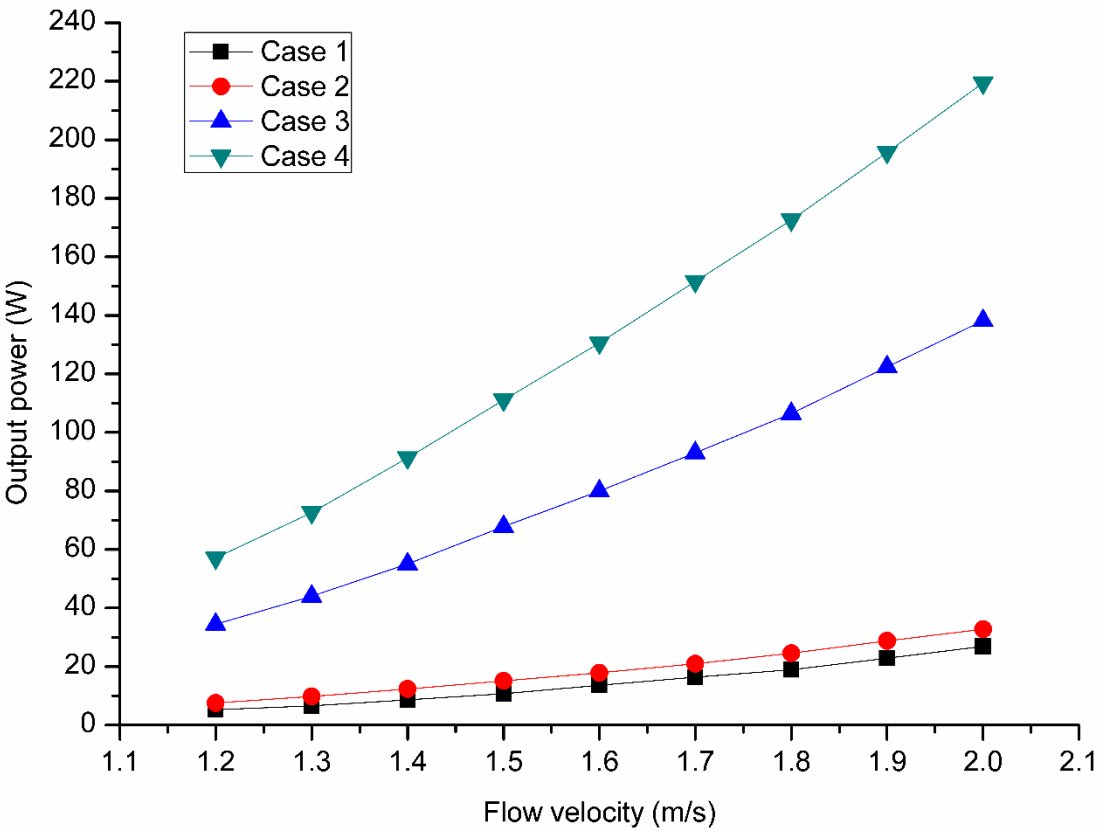

328

329 Fig.12 The output power of four cases on off-design points

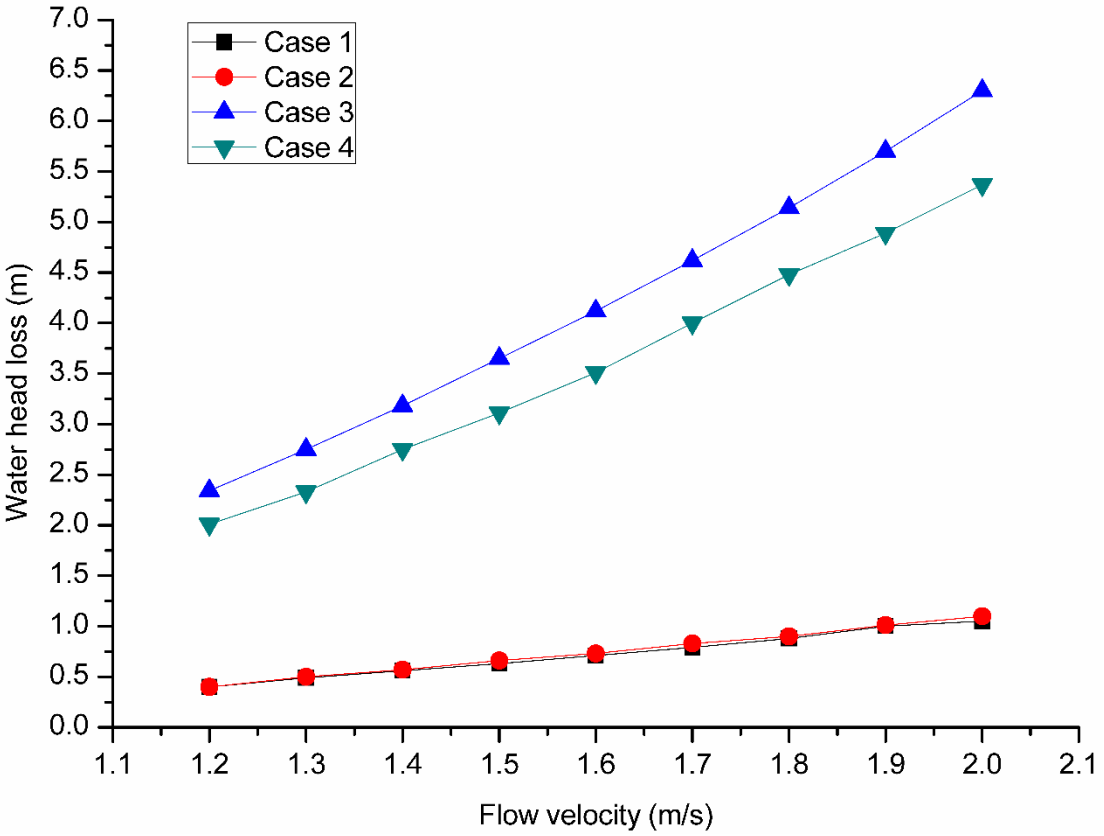

330

Fig.13 The water head loss of four cases on off-design points

3.2 Effects of tip clearance

As analyzed in the above part, the blocks can direct and concentrate the water flow to the advancing blades and cover the flow towards the returning blades. Therefore, the positive torque generated by the advancing blades can be enhanced while the negative torque of returning blades can be reduces. However, due to the tip clearance existing between the upstream block and the runner (as shown in Figure 14), the tip leakage may have a reverse impact on the turbine performance. In hydraulic machinery, tip clearance is a crucial parameter which influences the energy performance, flow patterns and Pressure fluctuation [33,34,35]. In this part, three models with different tip clearances (i.e. 10mm, 8mm and 5mm, respectively) were simulated for different TSR at the design point to study the effects of tip clearance on the turbine performance.

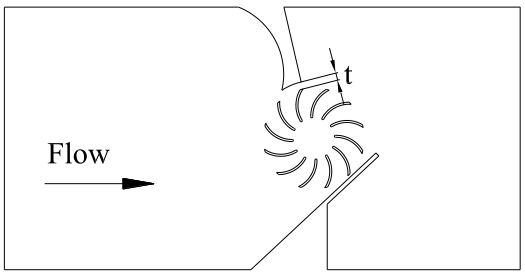

Fig.14 Tip clearance of the inline cross-flow turbine

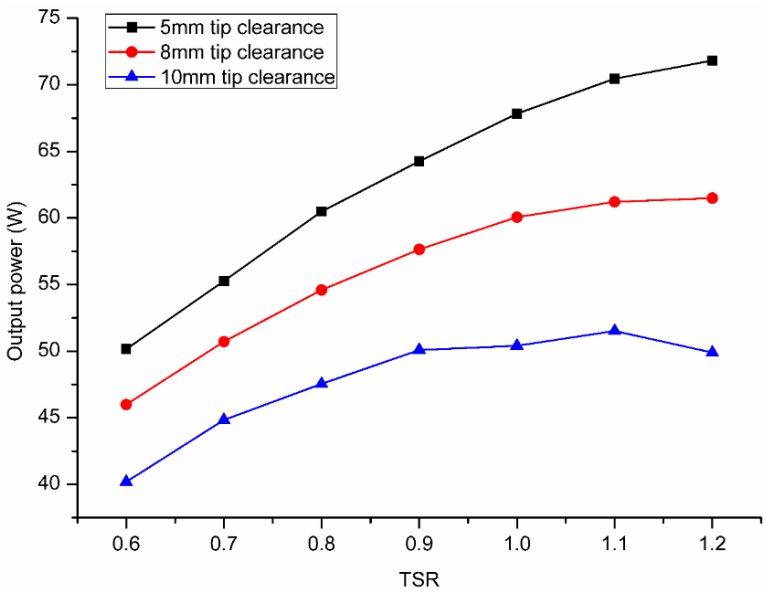

Fig.15 The output power of models with different tip clearance

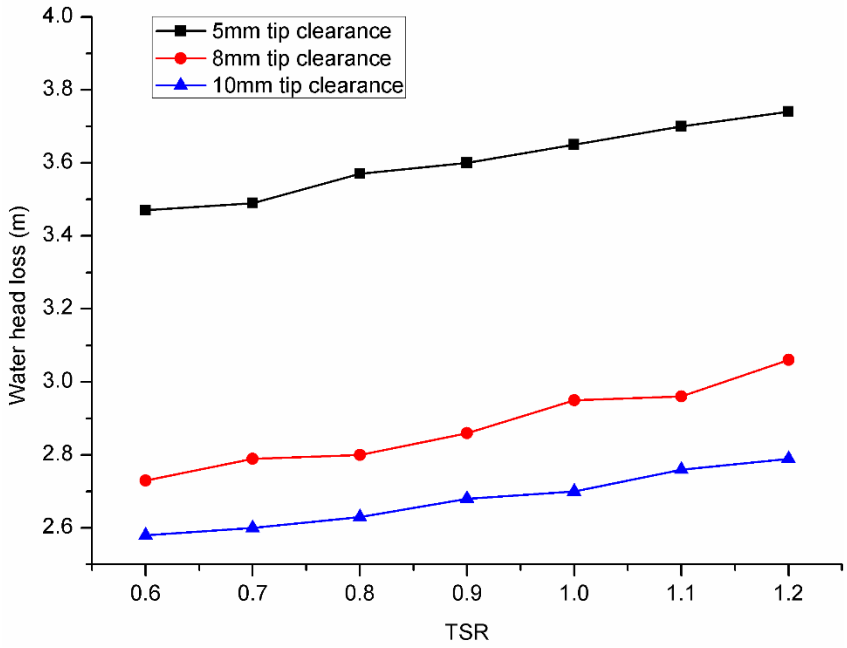

Fig.16 The water head loss of models with different tip clearance

The comparisons of output power and water head loss of models with different tip clearance obtained for different TSR are indicated in Figure 15 and 16. It can be observed that the output power variation of models with different tip clearances is relatively large. For example, on the design point, the maximum output power of model with 10mm tip clearance is only about 52W while that of the 5mm tip clearance model is more than 70W. On the other hand, although the water head losses of all models encounter a slight variation with the TSR, the head loss of 5mm tip clearance model is much larger than that of the other two models.

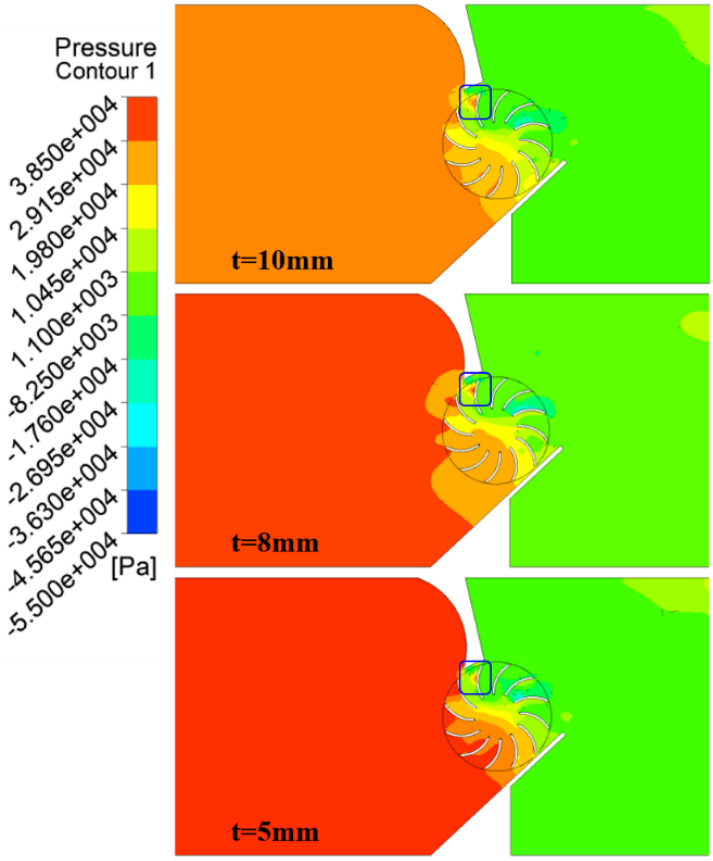

Fig.17 The pressure contours of models with different tip clearance

Figure 17 shows the pressure contour through the models with different tip clearance. It indicates that a high pressure region caused by the tip leakage exists on the back of returning blades, resulting in a negative torque on the runner. But by comparing the pressure contours, it is further seen that the smaller the tip clearance is, the lower pressure behind the returning blades will be. Besides, it is found that for a smaller tip clearance, the indicated pressure at the runner inlet side is larger. As a result, the pressure difference between the upstream side and the downstream side of the runner is larger and more water will be sucked to flow towards the advancing blades, therefore the turbine performance could be improved [36, 37].

In conclusion, the tip clearance mainly has two effects on the turbine performance. Firstly, a small tip clearance can reduce the tip leakage thus reduce the reversing torque on the returning blades. Secondly, for decreasing tip clearance, the pressure drop through the inlet and outlet of the runner will be increased, which draws more water to

flow through the runner and enhances the positive torque generated by the advancing blades. According to the above analysis, values of tip clearance less than 5mm are expected to further increase the turbine performance, but the manufacturing and assembling difficulties make it challenging to fabricate a prototype. Besides, the output power of model with 5mm tip clearance is enough for the power requirement of water leakage monitoring system, so the final tip clearance of this turbine is designed as 5mm.

3.3 Design of self-adjustable vane

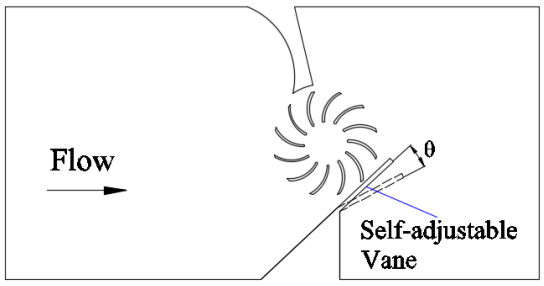

Fig.18 The schematic diagram of the self-adjustable vane

As requested by the Water Supplies Department of Hong Kong, the water head loss through the turbine cannot exceed 5m water. However, according to the results in part 3.1, the water head losses of the proposed design scheme at higher flow velocities have exceeded 5m water. To solve this problem, a self-adjustable vane located on the downstream side of the turbine was designed and tested. As shown in Figure 18 is the schematic diagram of the self-adjustable vane, in which a damping device (a torsional spring in the present study) is designed to control the opening degree of the self-adjustable vane. At low flow velocities (i.e. less and equal to 1.5m/s), the damping device can hold the self-adjustable vane at its original position, but when the flow velocity is more than 1.5m/s, the water will push the self-adjustable vane to open to some degree, so some water will flow through the space between the runner and the self-adjustable vane. With the increase of the flow velocities, the opening degree becomes larger. It is assumed that the opening degree of the self-adjustable vane at the flow velocity larger than 1.5m/s increases by 3° with every 0.1m/s. For example, the

395 opening degree at 1.6m/s is 3° while that at 2m/s is 15°.

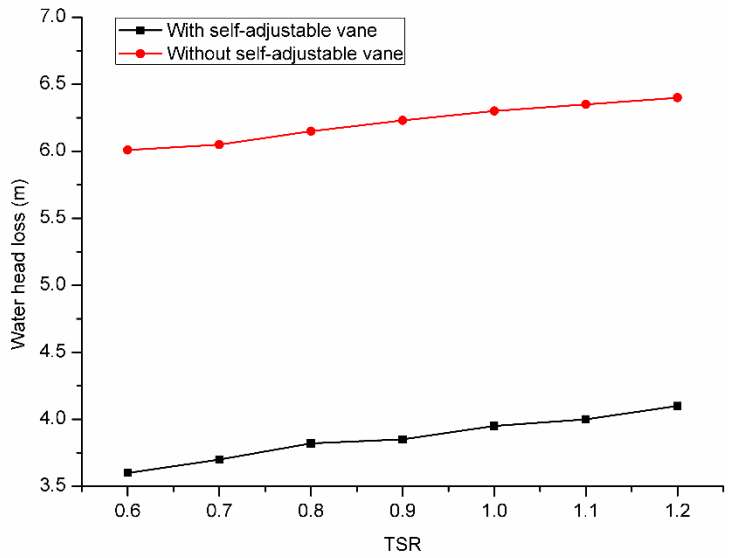

396

397 Fig.19 The water head loss of models with and without self-adjustable vane

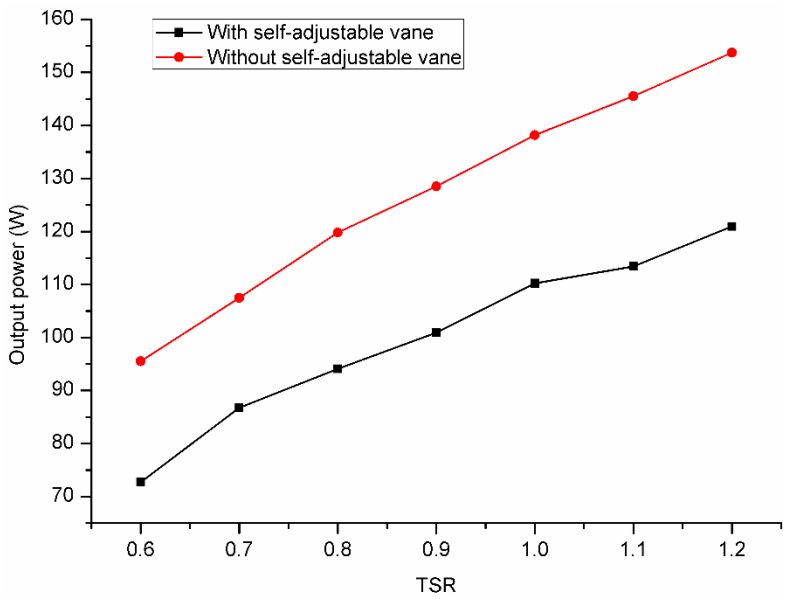

398

399 Fig.20 The output power of models with and without self-adjustable vane

400

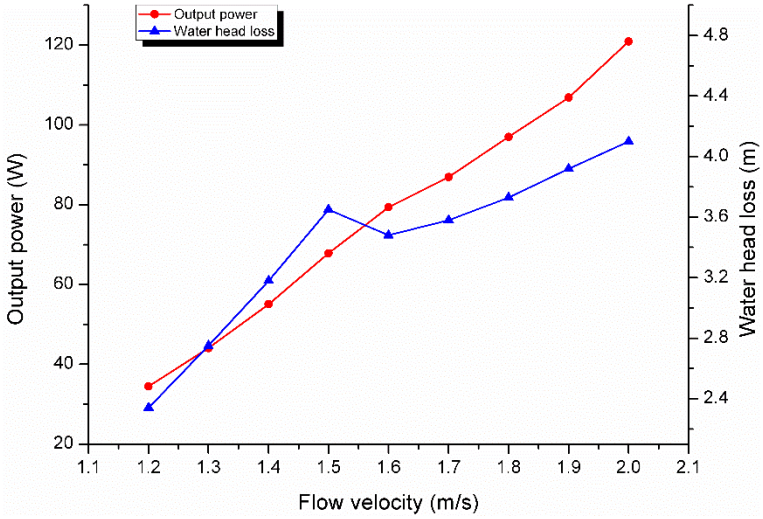

401

402 Fig.21 The off-design performance of turbine model with self-adjustable vane

403 The comparisons of water head loss and output power of models with and without self-
404 adjustable vane at flow velocity of 2.0m/s obtained for different TSR are indicated in
405 Figure 19 and 20. It can be observed that the water head loss reduced by about 3.5m
406 water while the output power reduced by nearly 30W after adopting the self-adjustable
407 vane, which means that the self-adjustable vane has a good performance in reducing
408 the water head loss. Although the output power also reduces with the opening of self-
409 adjustable vane, it is enough for the power requirement of water leakage monitoring
410 system. Besides, the reduction of output power can lighten the load on controller and
411 chargeable batteries. Figure 21 indicates the simulated turbine performance on off-
412 design points. Both the output power and water head loss increase with the increase of
413 the flow velocity, but the growth becomes slow at higher flow velocities. The water
414 head losses in the flow range from 1.2m/s to 2.0m/s are all less than 5m water, which
415 can satisfy the requirement of the Water Supplies Department very well. Besides, it can
416 also be observed that the minimum and the maximum output power are about 35W and
417 120W, which can not only meet power demand of water leakage monitoring system,
418 but also be within the tolerance capacity of the controller. In conclusion, the proposed
419 self-adjustable vane can avoid too much water head loss with little influence on the
420 output power.

4. Experimental results and analysis

Fig.22 The inline cross-flow turbine prototype

After a series of CFD simulation, the final configuration was determined and inline cross-flow turbine prototype was fabricated, as shown in Figure 22. The turbine is mainly composed of turbine body, runner, runner holder, upstream block, self-adjustable vane, shaft, mechanical seal and generator. Among them, the turbine body is a DN250 pipe with a length of 460mm. The runner is made of 12 blades, which are welded to 3 discs, in addition, a runner holder is located on the bottom of the turbine body to hold the terminal of the runner to reduce runner deformation. The main function of the runner is to harvest hydropower and transfer the generated torque to generator through the shaft. Both the upstream block and self-adjustable vane are manufactured by wire-electrode cutting and integrated with the turbine body by welding. The whole prototype is made of 316L stainless steel to avoid negative impacts on the water quality. Finally, the prototype was tested in the test rig to validate the simulation results and study its performance.

4.1 Validation of the numerical results

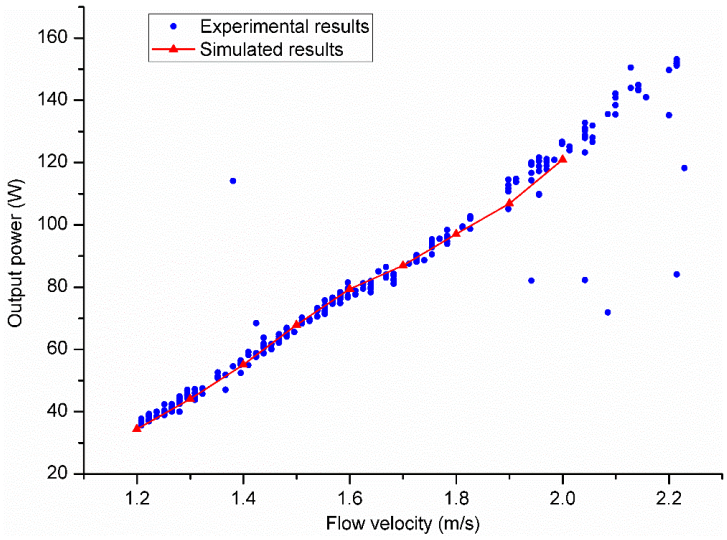

Fig.23 The comparison between experimental and numerical output power

Figure 23 and 24 show the comparison between the experimental and numerical results. The turbine prototype was tested over the flow velocities varying from 1.2m/s to 2.2m/s and the experimental data was recorded to compare with the computed results. It can be observed in Figure 22 and 23 that the simulated output power agrees very well with the measured values, but some difference exists between the simulated and experimental water head loss. The comparison between the numerical and the experimentally measured output power and water head loss is given in Table 3, the error percentage is also provided in the table. The measured output power on the design point is 69.1W with 2.62m water head loss, compared to the simulated values of 67.8W and 3.65m. Most of the error percentages in terms of output power are limited in ±5%. The error percentage of water head loss is relatively large and two main reasons may account for this phenomenon. Firstly, the CFD model is simplified, resulting in calculation uncertainties which are very difficult to be measured and ruled out. Secondly, the deviations can also be caused by experimental measuring errors. In the test rig, the unstable flow caused by the turbine may result in pressure fluctuation, which has significantly negative on measuring accuracy. However, the error values of water head loss are all less than 1m water. Hence, an acceptable good agreement between numerical

and experimental results was achieved.

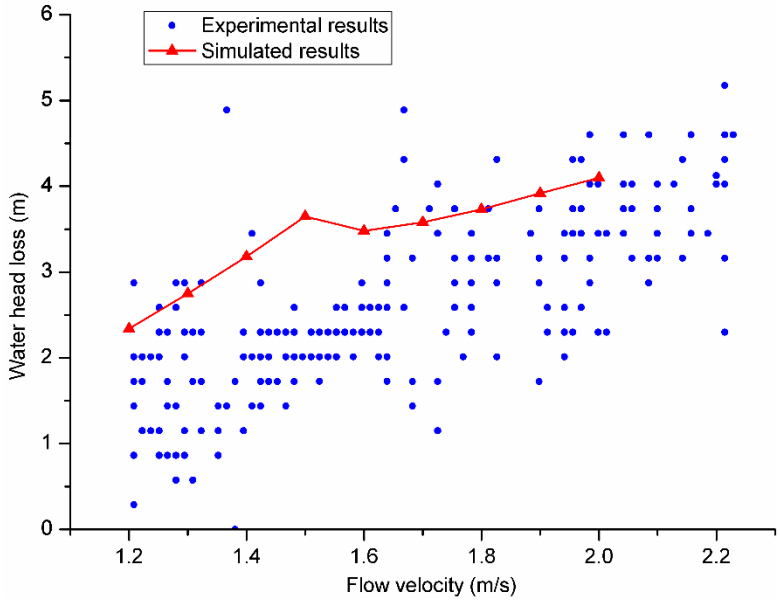

Fig.24 The comparison between experimental and simulation water head loss

Table 3 Comparison between computed and measured results

Flow velocity (m/s)	Output power (W)			Water head loss (m)		
	Experimental results	Simulation results	Error (%)	Experimental results	Simulation results	Error (%)
1.2	36.8	34.4	-6.5	2.01	2.34	16.4
1.3	43.2	44.0	1.85	2.11	2.75	30.3
1.4	53.4	55.1	3.18	2.23	3.18	42.6
1.5	69.1	67.8	-1.8	2.62	3.65	39.3
1.6	76.6	79.4	3.6	2.82	3.48	23.4
1.7	87.6	86.9	-0.8	3.32	3.58	7.8
1.8	94.6	97.0	2.5	3.10	3.73	20.3
1.9	105.7	106.8	1.0	3.95	3.92	-0.76
2	124.1	121.0	-2.5	3.91	4.10	4.8

4.2 Experimental performance of the turbine

The turbine prototype was tested at a flow velocity of 1.3m/s for 12 hours a day for one month to study its performance. Figure 25 shows the turbine performance in one typical day. The output power keeps very stable around 50W, and the battery charging voltage increases gradually then remains steady under 28V. Although the water head loss varies significantly with the time, the maximum value is still below 3m water. As described in

Figure 26 is the statistics of daily electricity generation in one month. The average daily electricity generation is about 600Wh, which ensures a constant power supply for almost any general monitoring system. Besides, as the tests were conducted at a flow velocity of 1.3 m/s while the actual flow velocity in the water pipe varies from 1.2m/s to 2 m/s, the turbine performance in practical application is expected to be better than the test results.

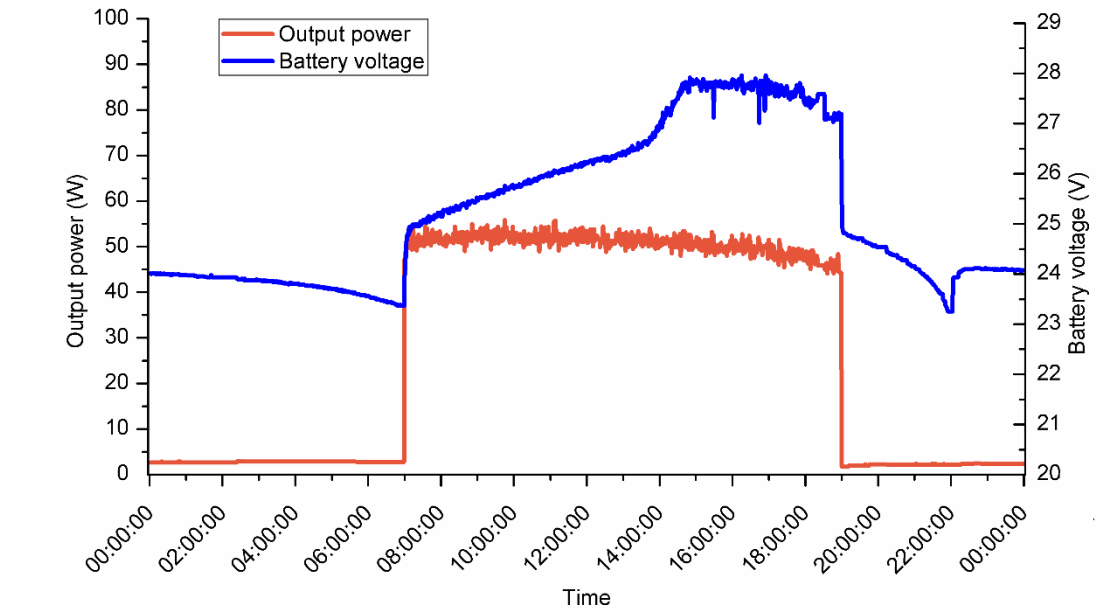

(a) Output power and battery charging voltage

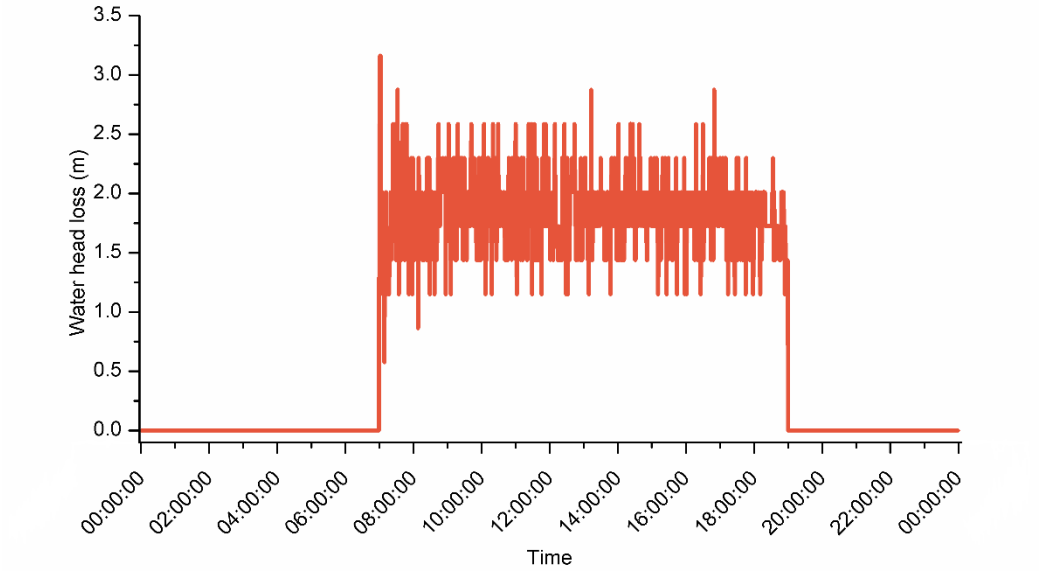

(b) Water head loss

Fig.25 The turbine performance in one typical day

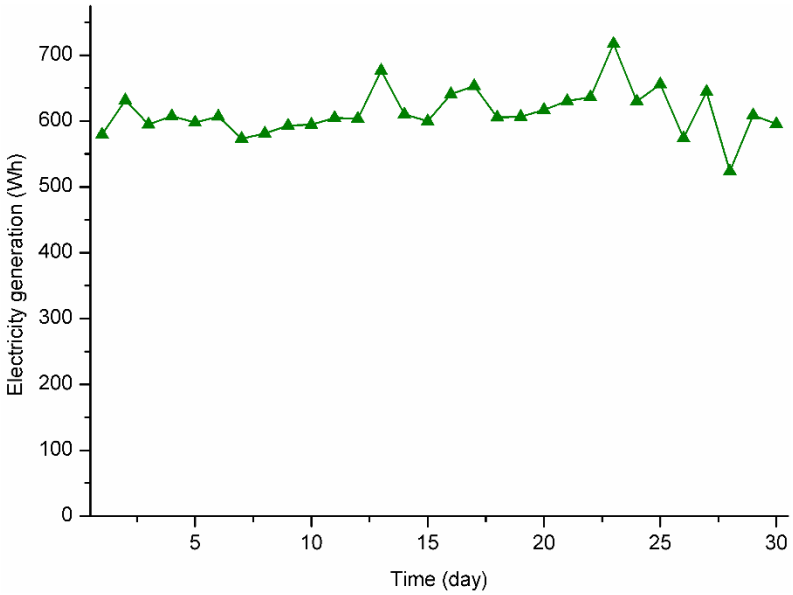

Fig.26 Daily electricity generation

Conclusion

This research presents the development of a novel inline vertical cross-flow turbine for hydropower generation in urban water mains by numerical and experimental methods. The flow field characteristics, output power and water head loss of the system have been analyzed to study the effects of block shape, tip clearance and self-adjustable vane on the turbine performance. As referred from the present study, the following conclusions can be obtained:

(1) The proposed upstream and downstream blocks can act as the nozzle and diffuser of a conventional cross-flow turbine to enhance the flow velocity and pressure difference through the runner.

(2) The configuration with an upstream concave block and a downstream plane block is suitable for the power demand of a water leakage monitoring system.

(3) A smaller tip clearance can reduce the tip leakage so that to reduce the reversing torque on the returning blades and increase the pressure drop through the runner. The turbine performance can thus be improved.

(4) The proposed self-adjustable vane achieves ideal performance in avoiding excess water head loss with little influence on the output power.

(5) The experimental results indicate that the numerical method used in the present research can predict the turbine performance with an acceptable accuracy and provide a good guidance for turbine design and improvement.

(6) The prototype test results show that the output power at the design point is 69.1W with 2.62m water head loss. Besides, over a flow velocity range varying from 1.2m/s to 2.2m/s, the water head loss is always below 5m water and the normal water supply is not affected.

(7) After a month-long test at the flow velocity of 1.3m/s, the prototype was proved very reliable with steady performance and its daily electricity generation is about 600Wh, which is sufficient for powering any general water leakage monitoring system in an urban environment.

Acknowledgement

The authors would appreciate the financial supports provided by the Innovation and Technology Fund of Hong Kong Special Administrative Region Government (Grant No.: ITS/032/13) and the help from the Water Supplies Department of the Hong Kong SAR Government.

Reference

[1] Chen J, Yang H X, Liu C P, et al. A novel vertical axis water turbine for power generation from water pipelines. Energy, 2013, 54: 184-193.

[2] Yue D, Tang S L. Sustainable strategies on water supply management in Hong Kong. Water and Environment Journal, 2011, 25(2): 192-199.

[3] Chen Y D. Sustainable development and management of water resources for urban water supply in Hong Kong. Water international, 2001, 26(1): 119-128.

[4] Li W, Ling W, Liu S, et al. Development of systems for detection, early warning, and control of pipeline leakage in drinking water distribution: A case study. Journal of Environmental Sciences, 2011, 23(11): 1816-1822.

[5] Xu Q, Liu R, Chen Q, et al. Review on water leakage control in distribution networks and the associated environmental benefits. Journal of Environmental Sciences, 2014, 26(5): 955-961.

[6] Mehajabin N, Razzaque M A, Hassan M M, et al. Energy-sustainable relay node deployment in wireless sensor networks. Computer Networks, 2016, 104: 108-121.

[7] Valera A C, Soh W S, Tan H P. Enabling sustainable bulk transfer in environmentally-powered wireless sensor networks. Ad Hoc Networks, 2017, 54: 85-98.

[8] Rosenbloom D, Meadowcroft J. Harnessing the Sun: Reviewing the potential of solar photovoltaics in Canada. Renewable and Sustainable Energy Reviews, 2014, 40: 488-496.

[9] Dondi D, Bertacchini A, Brunelli D, et al. Modeling and optimization of a solar energy harvester system for self-powered wireless sensor networks. IEEE Transactions on Industrial Electronics, 2008, 55(7): 2759-2766.

[10] Weimer M A, Paing T S, Zane R A. Remote area wind energy harvesting for low-power autonomous sensors. system, 2006, 2(1): 2.

[11] Myers R, Vickers M, Kim H, et al. Small scale windmill. Applied Physics Letters, 2007, 90(5): 054106.

[12] Akhtar F, Rehmani M H. Energy replenishment using renewable and traditional energy resources for sustainable wireless sensor networks: A review. Renewable and Sustainable Energy Reviews, 2015, 45: 769-784.

[13] Hao W S, Garcia R. Development of a digital and battery-free smart flowmeter. Energies, 2014, 7(6): 3695-3709.

[14] Hoffmann D, Willmann A, Göpfert R, et al. Energy harvesting from fluid flow in water pipelines for smart metering applications. Journal of Physics: Conference Series. IOP Publishing, 2013, 476(1): 012104.

[15] Du J, Yang H, Shen Z, et al. Micro hydro power generation from water supply system in high rise buildings using pump as turbines. Energy, 2017, 137: 431-440.

[16] Kaunda C S, Kimambo C Z, Nielsen T K. A technical discussion on micro hydropower technology and its turbines. Renewable and Sustainable Energy Reviews, 2014, 35: 445-459.

[17] Elbatran, A. H., et al. Operation, performance and economic analysis of low head micro-hydropower turbines for rural and remote areas: a review. Renewable and

Sustainable Energy Reviews, 2015, 43: 40-50.
[18] Paish O. Small hydro power: technology and current status. Renewable & Sustainable Energy Reviews, 2002, 6(6):537–556.
[19] Saftner D A, Hryciw R D, Green R A, et al. The use of wireless sensors in geotechnical field applications//Proceedings of the 15th annual Great Lakes geotechnical/geoenvironmental conference. 2008.
[20] Ferro L M C, Gato L M C, Falcão A F O. Design of the rotor blades of a mini hydraulic bulb-turbine. Renewable energy, 2011, 36(9): 2395-2403.
[21] Li Y, Song G, Yan Y. Transient hydrodynamic analysis of the transition process of bulb hydraulic turbine. Advances in Engineering Software, 2015, 90: 152-158.
[22] Sammartano V, Aricò C, Carravetta A, et al. Banki-michell optimal design by computational fluid dynamics testing and hydrodynamic analysis. Energies, 2013, 6(5): 2362-2385.
[23] Tan L, Cao S, Wang Y, et al. Direct and inverse iterative design method for centrifugal pump impellers. Proceedings of the Institution of Mechanical Engineers, Part A: Journal of Power and Energy, 2012, 226(6): 764-775.
[24] Xu Y, Tan L, Cao S, et al. Multiparameter and multiobjective optimization design of centrifugal pump based on orthogonal method. Proceedings of the Institution of Mechanical Engineers, Part C: Journal of Mechanical Engineering Science, 2017, 231(14): 2569-2579.
[25] Tan L, Zhu B, Cao S, et al. Influence of blade wrap angle on centrifugal pump performance by numerical and experimental study. Chinese journal of mechanical engineering, 2014, 27(1): 171-177.
[26] Zhang B, Liang C. A simple, efficient, and high-order accurate curved sliding-mesh interface approach to spectral difference method on coupled rotating and stationary domains. Journal of Computational Physics, 2015, 295(C):147-160.
[27] Ferrer E, Willden R H J. A high order Discontinuous Galerkin - Fourier incompressible 3D Navier-Stokes solver with rotating sliding meshes. Journal of Computational Physics, 2012, 231(21):7037–7056.
[28] Gourdain N. Prediction of the unsteady turbulent flow in an axial compressor stage. Part 1: Comparison of unsteady RANS and LES with experiments. Computers & Fluids, 2015, 106:119-129.
[29] Coroneo M, Montante G, Paglianti A, et al. CFD prediction of fluid flow and mixing in stirred tanks: Numerical issues about the RANS simulations. Computers & Chemical Engineering, 2011, 35(10):1959-1968.
[30] Moffat R J. Describing the uncertainties in experimental results[J]. Experimental thermal and fluid science, 1988, 1(1): 3-17.
[31] Acharya N, Kim C G, Thapa B, et al. Numerical analysis and performance enhancement of a cross-flow hydro turbine. Renewable energy, 2015, 80: 819-826.
[32] Elbatran A H, Ahmed Y M, Shehata A S. Performance study of ducted nozzle Savonius water turbine, comparison with conventional Savonius turbine. Energy, 2017.
[33] Liu Y, Tan L, Hao Y, et al. Energy performance and flow patterns of a mixed-flow

pump with different tip clearance sizes. Energies, 2017, 10(2): 191.
[34] Hao Y, Tan L, Liu Y, et al. Energy performance and radial force of a mixed-flow pump with symmetrical and unsymmetrical tip clearances. Energies, 2017, 10(1): 57.
[35] Xu Y, Tan L, Liu Y, et al. Pressure fluctuation and flow pattern of a mixed-flow pump with different blade tip clearances under cavitation condition. Advances in Mechanical Engineering, 2017, 9(4): 1687814017696227.
[36] Kirke B. Developments in ducted water current turbines. Tidal paper, 2006 (25-04).
[37] Ponta F, Dutt G S. An improved vertical-axis water-current turbine incorporating a channelling device. Renewable energy, 2000, 20(2): 223-241.